Stochastic resonance in an asymmetric Schmitt trigger

F. Marchesoni
Istituto Nazionale di Fisica della Materia, Università di Camerino, I-62032 Camerino, Italy
and Department of Physics, University of Michigan, Ann Arbor, Michigan 48109

F. Apostolico and S. Santucci
Dipartimento di Fisica, Università di Perugia and Istituto Nazionale di Fisica della Materia, I-06100 Perugia, Italy
(Received 27 May 1998; revised manuscript received 7 December 1998)

The stochastic response of a low-noise asymmetric Schmitt trigger is simulated numerically in the strong-drive subthreshold regime, where the amplitude of a sinusoidal input component is set large compared to the intensity of the noise component. The effect of the asymmetry on the *stochastic resonance* phenomenon is characterized in terms of both spectral properties and switch time distributions of the trigger output. The connection between stochastic resonance and synchronization in an asymmetric bistable system is thus assessed on a quantitative basis. [S1063-651X(99)07504-2]

PACS number(s): 05.40.Ca, 85.30.De

I. INTRODUCTION

The Schmitt trigger (ST) [1] provides an ideal playground for both theorists and experimenters grappling with the phenomenon of *stochastic resonance* (SR) [2–7]. Typically, the ST input consists of two components, whose amplitudes greatly depend on the experimental circumstances: (i) a noisy signal with zero mean and finite correlation time; (ii) one or more embedded periodic signals with arbitrary waveforms. Let us consider for simplicity input signals $x(t)$ of the form

$$x(t)=\xi(t)+A_0\cos(\Omega t+\phi), \tag{1.1}$$

where $\xi(t)$ is a zero-mean stationary Gaussian noise with intensity (standard deviation) σ and autocorrelation function

$$\langle \xi(t)\xi(0)\rangle=\sigma^2 e^{-|t|/\tau}. \tag{1.2}$$

Throughout this work $\xi(t)$ is assumed to be short-time correlated compared with the modulation, that is $\Omega\tau\ll 1$. The trigger output rests in state—as long as the input $x(t)$ is smaller than a threshold value $b(1+\epsilon)$. As $x(t)$ crosses $b(1+\epsilon)$ the trigger switches (almost) instantaneously into state $+$ and sits there as long as $x(t)>-b(1-\epsilon)$. The ST output is a dichotomic signal with values $\pm y_m$; in the following y_m is set to one for convenience. The parameter ϵ (with $\epsilon\geqslant 0$) quantifies the asymmetry of the device and of its output. Of course, the modulation of the input signal (1.1) drives a periodic output component $\langle y(t)\rangle$ with the same period $T_\Omega=2\pi/\Omega$. In the *subthreshold* regime $A_0<b(1-\epsilon)$ with $\Omega\tau\ll 1$, the trigger switches are noise-assisted random events that occur with time constants $T_\mp(\sigma,\epsilon)=T_0[b(1\pm\epsilon)]$ from the $\mp$ to the $\pm$ state, where the spontaneous switch time $T_0(b)$ with $A_0=0$ reads [7]

$$T_0(b)=\frac{\tau\sqrt{\pi}}{1+\Phi(\bar{b})}\int_{-\infty}^{\bar{b}} e^{x^2}[1+\Phi(x)]^2dx, \tag{1.3}$$

with $\Phi(x)=(2/\sqrt{\pi})\int_0^x e^{-z^2}dx$ and $\bar{b}=b/\sqrt{2\sigma^2}$. At small noise intensities $\sigma\ll b$ our result (1.3) approaches $T_0(b)=\tau\sqrt{2\pi}(\sigma/b)\exp(b^2/2\sigma^2)$, whereas the opposite limit $\sigma\gg b$ yields $T_0(b)=\tau\ln 2$. These analytical predictions for $T_\pm$ are valid under the linear response theory restriction $A_0 b/\sigma^2\ll 1$, only, as one can verify by replacing b with $b\mp A_0\cos(\Omega t+\phi)$ in $T_0[b(1\pm\epsilon)]$ and, then, expanding in powers of A_0. However, experimenters are mostly concerned with the opposite limit $A_0 b/\sigma^2\gg 1$, meaning that the periodic component of the input signal dominates over the device noise, no matter what its source(s) [3].

In the following we concentrate on the case of a subthreshold ST with $(\sigma/b)^2\ll A_0/b<1$ and $\Omega\tau\ll 1$. The consequences of such an assumption are twofold: (i) Nonlinear effects become appreciable, so that the dependence of the switch times $T_\pm$ on the forcing amplitude A_0 is no longer negligible; (ii) The instantaneous switch times $T_\pm(t)$ are modulated in time with relatively large amplitudes [4], as proven by the inequality

$$\max\left|\frac{dT_\pm}{dt}\right|\sim(A_0 b/\sigma^2)\Omega T_\pm\gg 1, \tag{1.4}$$

which holds true throughout the entire parameter domain relevant to SR, but for extremely low frequencies. In our numerical investigation we set A_0, σ and Ω so as to verify the *strong drive* condition (1.4).

Symmetric ($\epsilon=0$) subthreshold ST have been investigated extensively [3–7] in connection with SR, a phenomenon where the amplitude of the output driven component peaks at a certain value of the noise intensity. As a main advantage with respect to the continuous bistable systems studied in the earlier literature, the output of a ST is entirely controlled by the switching mechanism, whereas in a continuous bistable system interwell and intrawell dynamics are at times hard to unravel [2]. For this reason the conclusions of our investigation are expected to apply to any asymmetric bistable system.

In the present work we report and discuss the results of detailed numerical simulations of strongly driven subthreshold ST with special focus on (i) the differences between the weak and strong drive limit (Sec. II); (ii) the effects of the

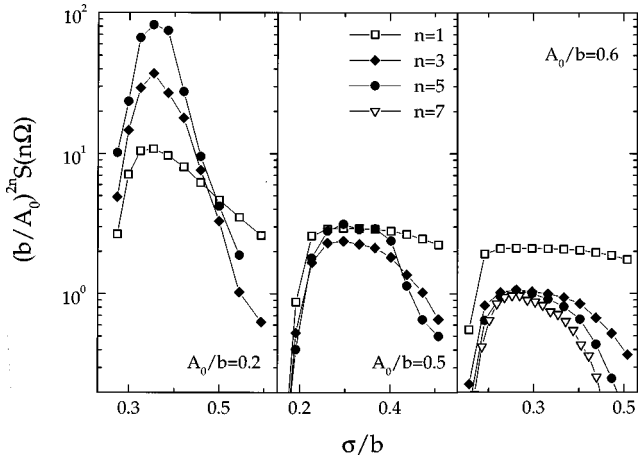

FIG. 1. Spectral peak strengths $S(n\Omega)$ vs noise intensity σ/b for different values of A_0/b. Simulation parameters: $\epsilon=0$ and $\Omega\tau=1.25\times10^{-2}$; time and signal scales: $\tau=2\times10^{-5}$ s and $b=200$ (arbitrary units).

asymmetry on the detectability and characterization of SR in terms of either output spectral properties (Sec. III) or appropriate switch time distributions (Sec. IV); (iii) the synchronization mechanism underlying the onset of SR in an asymmetric bistable device (Sec. IV).

II. STRONG-DRIVE SYMMETRIC REGIME

Let us consider first the case of SR in a symmetric ($\epsilon=0$) subthreshold ST driven by a relatively strong periodic modulation (1.1) with $(\sigma/b)^2 \ll A_0/b < 1$. In order to explore the main differences with the better known linear regime [2] $A_0/b \ll (\sigma/b)^2 \ll 1$, we discuss here simulation evidence of SR according to two alternative schemes, namely, the spectral and the synchronization-based characterizations.

A. Spectral characterization

This is the most widespread characterization of the SR phenomenon [2]. One computes the phase-averaged power spectral density $S(\omega)$ of the system output $y(t)$ and verifies that δ-like spectral peaks appear at integer multiples of the forcing frequency Ω. In the symmetric case a rigorous selection rule allows spectral peaks at odd Ω multiples, only. In Fig. 1 the strength of such peaks (that is, the integral of the relevant δ-like spectral peaks) $S(n\Omega)$ is plotted versus the noise intensity σ at fixed frequency and for increasing values of the amplitude A_0. New interesting spectral properties become apparent. (i) All *odd* spectral peaks exhibit SR behavior and, most notably, the resonance seems to take place for the same value of σ/b (contrary to the weakly driven case [8]). (ii) No low noise ''shoulder'' in the resonance curve of $S(n\Omega)$ versus σ is observable, at variance with the results of Ref. [9] for a continuous system. This means that such an effect ought to be ascribed to the intrawell dynamics (totally absent in the present case), rather than to a desynchronization mechanism (the subharmonic ''wait loops'' of Ref. [9]). (iii) The resonance curves of $S(n\Omega)$ versus σ seem to scale as $(A_0/b)^{2n}$ to compare with the scaling law $(A_0/\sigma)^{2n}$ predicted in linear response theory approximation [2,8]: The noise controlled amplification mechanism grows negligible in the strong drive regime.

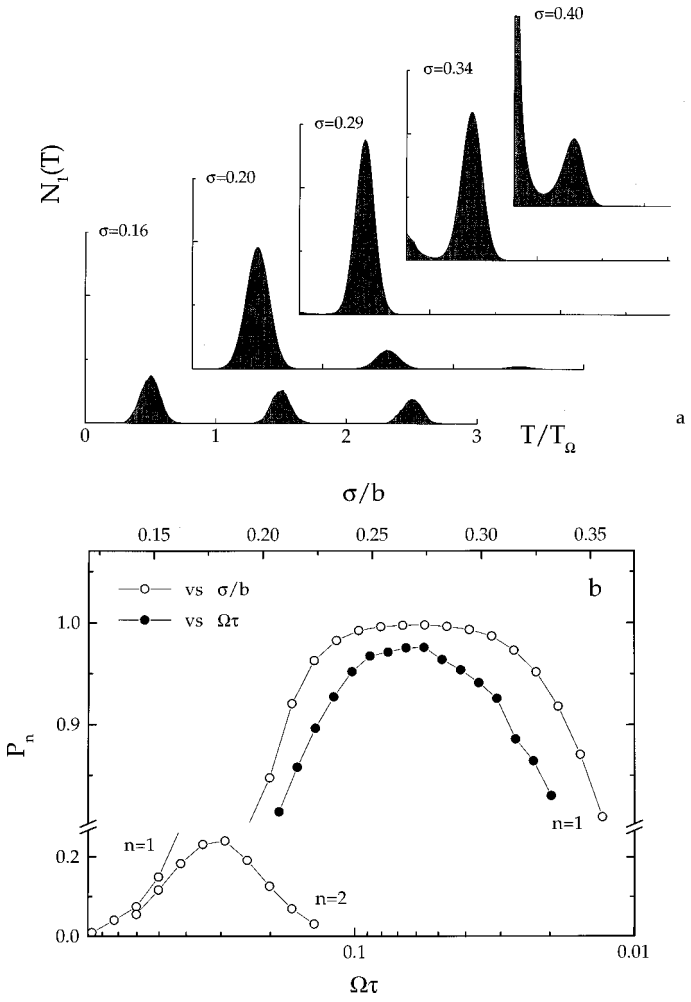

FIG. 2. (a) Residence time distributions $N_1(T)$ for $\Omega\tau=1.25\times10^{-2}$, $A_0/b=0.5$, and different values of σ/b. (b) $N_1(T)$ peak strengths P_1 and P_2 vs σ/b (at $\Omega\tau=1.25\times10^{-2}$) and P_1 vs $\Omega\tau$ (at $\sigma/b=0.37$) for $\alpha=0.25$ and after background subtraction. The remaining parameters are as in Fig. 1.

B. Synchronization-based characterization

An alternative characterization of SR was proposed in Ref. [10] by studying the normalized residence time distributions $N_1(T)$. One determines (numerically or experimentally, alike) the sequence of the time intervals between consecutive switches in opposite directions $\mp\rightarrow\pm\rightarrow\mp$: these are the residence times of the trigger in the $\pm$ state, respectively. Since in the symmetric case the average residence times in the $\pm$ state $\langle T_\pm\rangle$ coincide, here the residence time sequence needs not be sorted out according to the switch direction. In Fig. 2(a) we display an example of such residence time distributions $N_1(T)$ for fixed Ω but increasing σ values. As discussed in Refs. [10] and [2] the profile of $N_1(T)$ changes from a multipeaked structure at small noise intensity (tightly modulation-driven switches) to an exponential background (of random switches), through a maximum synchronization condition characterized by a single-peaked distribution. The nth N_1 peak is centered at $T_n=(n+1/2)T_\Omega$ and its strength [10]

$$P_n(\sigma,\Omega)=\int_{T_n-\alpha T_\Omega}^{T_n+\alpha T_\Omega} N_1(T)\,dT, \quad n=1,2,\ldots, \qquad (2.1)$$

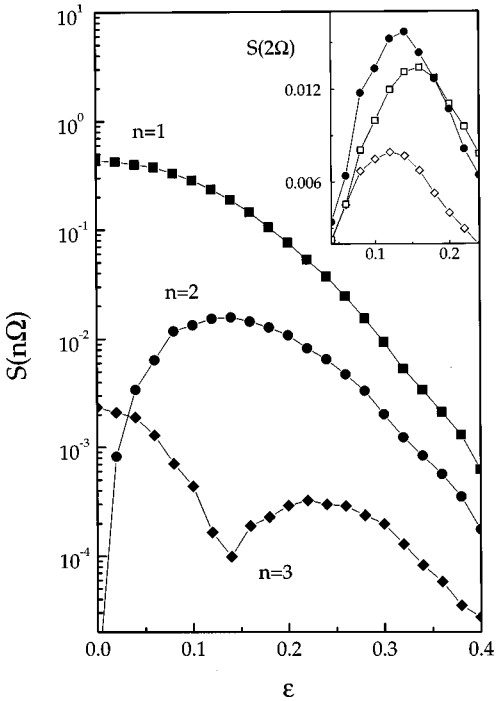

FIG. 3. Spectral peak strengths $S(n\Omega)$ vs the asymmetry parameter ϵ for $\sigma/b=0.35$, $\Omega\tau=1.25\times10^{-2}$, and $A_0/b=0.2$. Time and signal scales are as in Fig. 1. Inset: $S(n\Omega)$ vs ϵ for $\sigma/b=0.31$ (lozenges), $=0.35$ (circles), $=0.39$ (squares). The remaining parameters are unchanged.

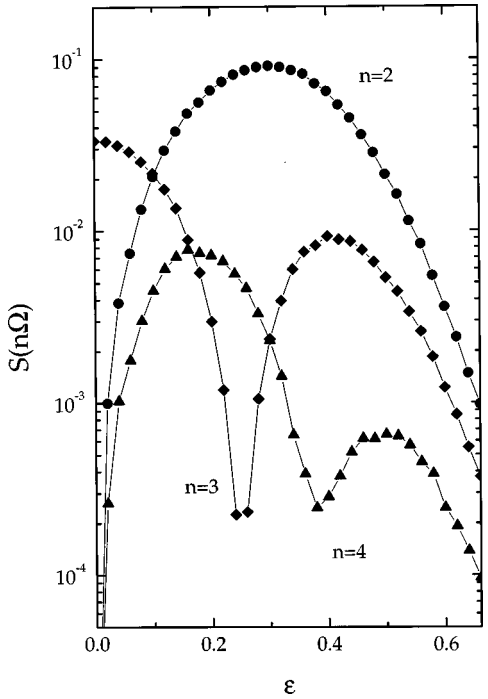

FIG. 4. Spectral peak strengths $S(n\Omega)$ vs the asymmetry parameter ϵ for $\sigma/b=0.37$, $\Omega\tau=1.25\times10^{-2}$, and $A_0/b=0.5$. Time and signal scales are as in Fig. 1.

with $0<\alpha\leqslant 1/4$, exhibits SR behavior both as a function of σ (at fixed Ω) and of Ω (at fixed σ). The σ and Ω dependence of P_1 is shown in Fig. 2(b). Here (and in Fig. 8), the random-switch background has been first blown up by taking the logarithm of the residence time distributions and then subtracted by means of a standard linear fitting algorithm. The choice of the σ/b axis origin and the orientation of the logarithmic $\Omega\tau$ axis are motivated by purely typographical reasons.

On anticipating the conclusions of Secs. III and IV, we remark that the resonant behaviors of $P_1(\sigma,\Omega)$ are a signature of the optimal temporal synchronization between driving signal, with period T_Ω, and switch sequence, with correlation time $\langle T_\pm\rangle$, which sets in at SR. In view of the scales chosen for σ/b and $\Omega\tau$ in Fig. 2(b), the time constant matching implied by SR as well as the existence of a maximum synchronization distribution $N_1(T)$ in Fig. 2(a) are apparent. Therefore, in the case of a strongly driven subthreshold ST the synchronization-based definition of SR is sound both qualitatively and quantitatively—i.e. the criticisms of Ref. [11] do not apply.

III. ASYMMETRY AND SPECTRAL PROPERTIES

In our model of Sec. I the ST asymmetry is controlled through the nonnegative parameter ϵ. The first question, now, is to assess how asymmetry affects the spectral characterization of SR. Of course, in the asymmetric regime the *even* peaks of the output power spectral density are not suppressed and, as one might expect, their strength exhibits SR behavior when plotted as a function of the noise intensity [2,8]. However, the dependence of $S(n\Omega)$ on the asymmetry parameter ϵ deserves particular attention. In Figs. 3 and 4 we display $S(n\Omega)$ versus ϵ for two values of the forcing amplitude and fixed noise intensities. Such noise intensities have been chosen in order to enhance the main features of the ϵ dependence of the curves on display, namely: (i) $S(\Omega)$ peaks at $\epsilon=0$, only; the spectral strengths $S(n\Omega)$ with $n>1$ show one or more peaks for $\epsilon>0$. The number of the maxima of $S(n\Omega)$ versus ϵ is $[(n+1)/2]$, i.e., the integer part of $n+1/2$ [6]. (ii) The peaks of each curve $S(n\Omega)$ versus ϵ attain their maximum at an optimal value of the noise intensity, simultaneously. The optimal noise intensity turns out to be the same for all the harmonics $n\Omega$, with the exception of the fundamental frequency Ω. (iii) The fundamental peak strength $S(\Omega)$ tends to be the most pronounced at a smaller noise intensity. This property of the higher harmonics peak strengths becomes clearly visible at large amplitudes (compare Fig. 3 to Fig. 4).

We tried to explain the number and the position of the maxima of $S(n\Omega)$ (Figs. 3 and 4) in terms of the synchronization scheme of Ref. [6] (for the weak drive regime see Ref. [8]). To this purpose we have computed the average residence times $\langle T_\pm\rangle$ in the $\pm$ state for the corresponding values of A_0 and σ (Figs. 5 and 6). Note that the average residence times $\langle T_\pm\rangle$ amount to an explicit computation of the switch times $T_\pm$ introduced in Sec. II. The synchronization argument of Ref. [6] runs as follows: The nth coefficient of the Fourier series of a *deterministic* asymmetric square wave with period T_Ω hits a maximum when

$$\langle T_+\rangle+\langle T_-\rangle=T_\Omega \tag{3.1}$$

and

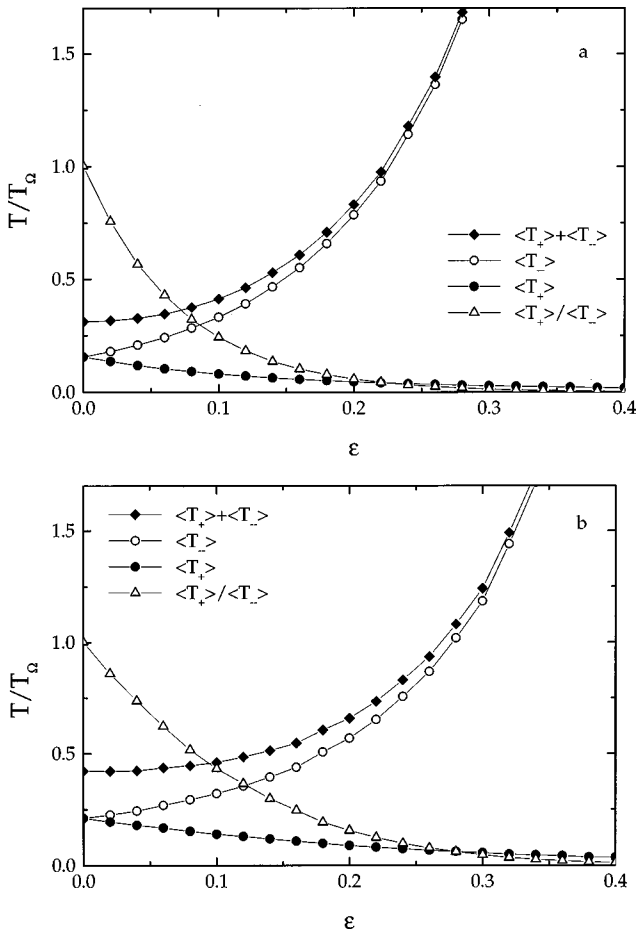

FIG. 5. Average residence times $\langle T_{\pm}\rangle$ vs ϵ for $\sigma/b=0.35$, $\Omega\tau=1.25\times10^{-2}$, and $A_0/b=0$ (a), $=0.2$ (b). Time and signal scales are as in Fig. 1.

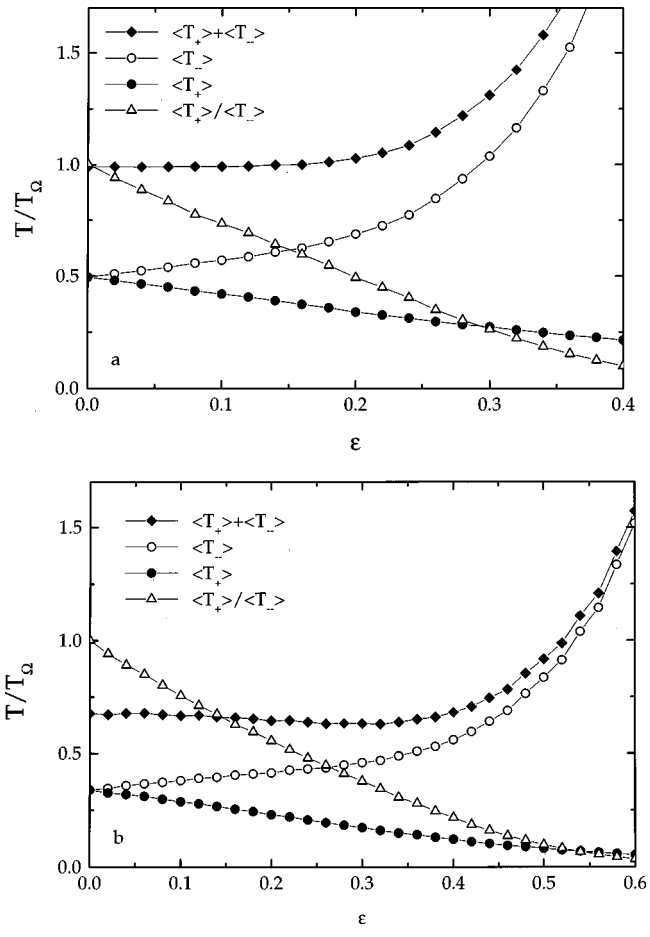

FIG. 6. Average residence times $\langle T_{\pm}\rangle$ vs ϵ for $\Omega\tau=1.25\times10^{-2}$, $A_0/b=0.5$, and $\sigma/b=0.29$ (a), $=0.37$ (b). Time and signal scales are as in Fig. 1.

$$\frac{\langle T_+\rangle}{\langle T_-\rangle}=\frac{m}{2n-m}, \tag{3.2}$$

where m is odd and $1\leqslant m\leqslant n$. In condition (3.1) synchronization is assumed and $\langle T_{\pm}\rangle$ are taken as the time duration of the positive/negative mode of the square wave. Condition (3.2) is a trigonometric consequence of the synchronization requirement (3.1). For the *stochastic* output of a subthreshold noisy ST, the solutions of Eqs. (3.1) and (3.2) have been advocated to locate the maxima of $S(n\Omega)$ in the (σ,ϵ) plane [6].

The picture that emerges from our simulation study agrees only in part with the argument of Ref. [6]. First of all, we confirm that the trigonometric condition (3.2) seems to predict well the number $[(n+1)/2]$ of the maxima of the curves $S(n\Omega)$ versus ϵ. As far as the position of the maxima on the ϵ axis is concerned, condition (3.2) works better and better at increasingly large forcing amplitudes and more accurately for the maxima at low ϵ values. The readers can verify for themselves the above statements by collating Figs. 3–6. The validity of the synchronization condition (3.1) is more dubious. It holds good for the maximum of $S(\Omega)$ at $\epsilon=0$ and only for large forcing amplitudes [compare Figs. 5(b) and 6(a)]. Note that for $n=1$ and $\epsilon=0$ the trigonometric condition is automatically satisfied due to the reflection symmetry of the output $y(t)$. Now, let us restrict our discussion to Figs. 4 and 6, where conditions (3.1) and (3.2) are more likely to apply. The maxima of $S(n\Omega)$ with $n>1$ versus ϵ are the most prominent at one optimal noise intensity, substantially larger than the optimal noise intensity for $S(\Omega)$. The corresponding residence times $\langle T_{\pm}\rangle$ at the optimal σ values for $n=0$ and $n>1$ are plotted in Fig. 6. The position of the maxima of $S(n\Omega)$ displayed in Fig. 4 is closely determined by condition (3.2), whereas $\langle T_+\rangle+\langle T_-\rangle$ is indeed constant throughout the ϵ range of interest (within the statistical accuracy of our simulation), but appreciably smaller than T_{Ω}.

In conclusion, the trigonometric condition (3.2) holds true under the weaker constraint that

$$\langle T_+\rangle+\langle T_-\rangle=\text{const.} \tag{3.3}$$

The differential version of condition (3.3) at $\epsilon=0$, $d\langle T_+\rangle/d\epsilon|_0=d\langle T_-\rangle/d\epsilon|_0$ yields an estimate for the optimal noise intensity of the maxima of $S(n\Omega)$ versus ϵ, whereas the trigonometric condition (3.2) at the optimal noise intensity pinpoints the position of the $S(n\Omega)$ maxima on the ϵ axis. Conditions (3.1) and (3.3) seem to render quite closely the results of our numerical simulation in the strong drive regime.

IV. RESIDENCE TIME DISTRIBUTIONS

We try, now, to characterize SR in terms of residence time distributions. In the asymmetric case $N_1(T)$ should be

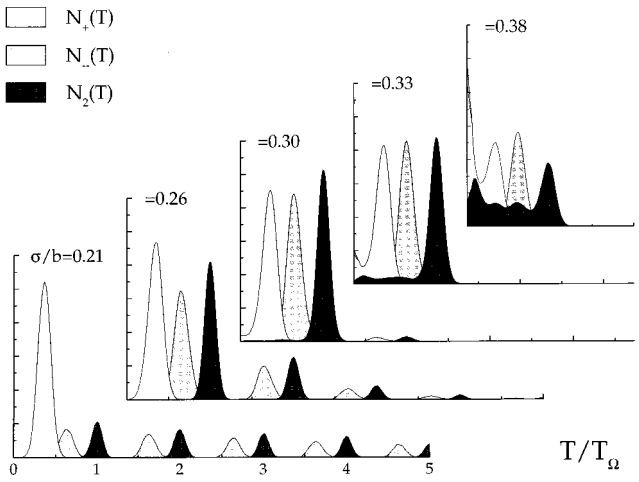

FIG. 7. Residence time $N_{\pm}(T)$ and return time distributions $N_2(T)$ for $\Omega\tau=1.25\times10^{-2}$, $A_0/b=0.5$, $\epsilon=0.2$ and different values of σ/b. Time and signal scales are as in Fig. 1.

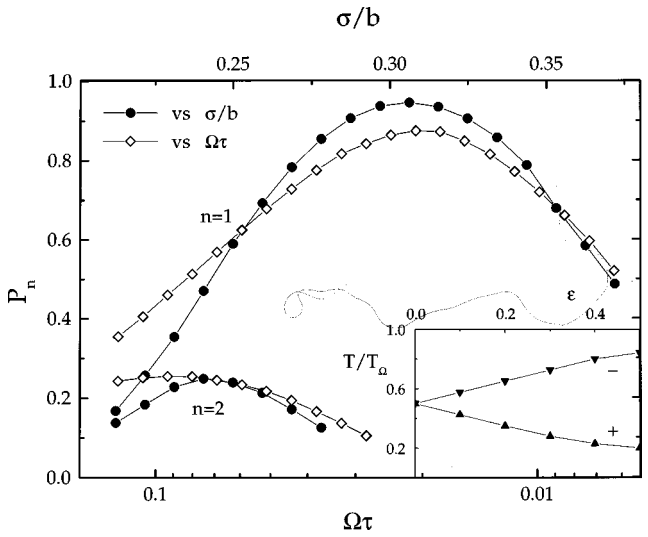

FIG. 8. $N_2(T)$ peak strengths P_1 and P_2 vs σ/b (at $\Omega\tau=1.25\times10^{-2}$) and vs $\Omega\tau$ (at $\sigma/b=0.30$) for $\alpha=0.5$ and after background subtraction. The remaining parameters are as in Fig. 7. Inset: position of the the first peak of $N_{\pm}(T)$ vs ϵ at $\sigma/b=0.37$. The remaining parameters are as in Fig. 7.

replaced by a distribution $N_+(T)$ for the residence times in the state $+$ and a distribution $N_-(T)$ for the residence times in the state $-$, with $N_+(T)\neq N_-(T)$ for $\epsilon\neq0$. It follows that, as pointed out by Jung [2,12], the synchronization criterion of Sec. II B cannot be carried over to the asymmetric case without modification.

Let us discuss first our results for the symmetric case displayed in Fig. 2(b). We verified that the maxima of the resonance curves of P_1 and P_2 versus σ/b correspond to the synchronization conditions $\langle T_{\pm}\rangle=(1/2)T_\Omega$ for P_1 [see also Fig. 6(a)] and $\langle T_{\pm}\rangle=(3/2)T_\Omega$ for P_2. Analogously, the curve of P_1 versus $\Omega\tau$ peaks at a forcing frequency such that $T_\Omega=2\langle T_{\pm}\rangle$. The interpretation of these results is detailed in Refs. [10] and [2]: due to the forcing action of the input periodic component, the ST tends to reside in either state for time intervals of the order of $(n+1/2)T_\Omega$; the nth peak of the $N_1(T)$ distributions attains its maximum strength when $(n+1/1)T_\Omega$ and $\langle T_{\pm}\rangle$ come close to one another, hence the maxima of P_n versus both σ/b and $\Omega\tau$.

For $\epsilon=0$ the distributions $N_{\pm}(T)$ coincide with $N_1(T)$; this is not the case for $\epsilon\neq0$, as clearly shown in Fig. 7. The properties of $N_{\pm}(T)$ can be easily explained, at least qualitatively:

(i) On increasing the asymmetry parameter ϵ, the first peak of $N_{\pm}(T)$ shifts to the left and to the right, respectively. The distance between the first peak of $N_-(T)$ and $N_+(T)$ increases linearly with ϵ (inset Fig. 8). This is an obvious consequence of the fact that for $\epsilon>0$ the switches from state $+$ to state $-$ are anticipated with respect to the switches in the opposite direction. (ii) Adjacent peaks of $N_{\pm}(T)$ are separated by a constant interval of the order of T_Ω, as is the case for $\epsilon=0$. In other words the peak structures of $N_{\pm}(T)$ shift rigidly in opposite directions. (iii) The peak structures of $N_{\pm}(T)$ change with varying the noise intensity and/or the forcing frequency in a fashion that closely resembles the SR behavior of $N_1(T)$ in the symmetric case; however, the resonant synchronizations of $N_{\pm}(T)$ occur for different values of σ/b and $\Omega\tau$.

Property (iii) of $N_{\pm}(T)$ makes the synchronization criterion of Sec. II B untenable for an asymmetric ST. To avoid such a difficulty we make use of the *return time* distribution $N_2(T)$ [13,14]: here, the time interval T denotes the time separation between two subsequent switches in the same direction (say, from state $-$ to state $+$). The choice of the switch direction is statistically immaterial, even for an asymmetric device. Moreover, two subsequent switches in one direction are always separated by one switch in the opposite direction (say, from state $+$ to state $-$). No surprise that the peaks of $N_2(T)$ in Fig. 7 are centered at nT_Ω and that $N_2(T)$, too, evolves from a multipeaked structure for low noise intensities (high forcing frequencies) to the superposition of a prominent peak at T_Ω and an exponential background for relatively large noise intensities (low forcing frequencies). The onset of two additional peaks in correspondence with the first peaks of $N_{\pm}(T)$ (only one in the symmetric case!) is a peculiarity of all bistable devices; since it shows up at noise intensities well above the relevant SR range, we leave the investigation of this property of the return time distributions (unnoticed in the earlier literature [13,14]) to a forthcoming publication.

It follows immediately from the preceding discussion that the synchronization-based characterization of SR can be carried out consistently in terms of $N_2(T)$, as well. Here, the nth peak strength is defined by

$$P_n(\sigma,\Omega)=\int_{T_n-\alpha T_\Omega}^{T_n+\alpha T_\Omega} N_2(T)\,dT, \quad n=1,2,\ldots, \qquad (4.1)$$

with $T_n=nT_\Omega$ and $0<\alpha\leqslant1/2$. In Fig. 8 we display the N_2 peak strengths P_1 and P_2 against the noise intensity at fixed forcing frequency, and vice versa, for $\epsilon=0.2$. The maxima of the curves thus obtained correspond to the synchronization condition $\langle T_+\rangle+\langle T_-\rangle=T_\Omega$ for P_1 and $\langle T_+\rangle+\langle T_-\rangle=2T_\Omega$ for P_2, as expected.

Finally, we verified that the synchronization criterion of this section applies well to forcing amplitudes A_0/b as small

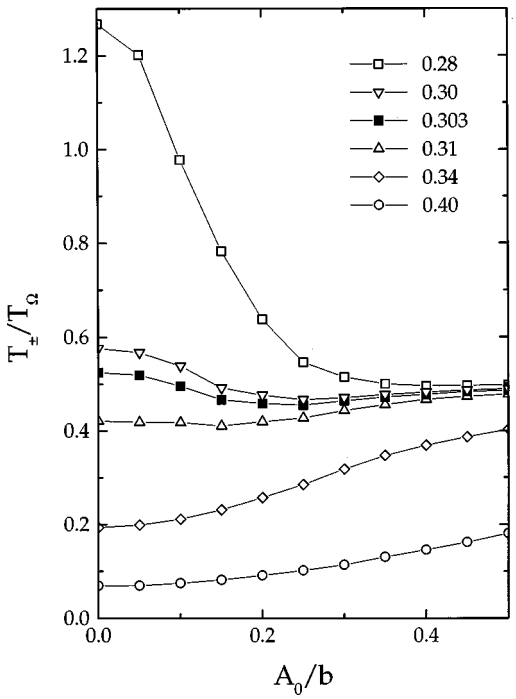

FIG. 9. Average residence times $\langle T_\pm \rangle$ as a function of A_0 for different values of σ/b and $\epsilon=0$. The remaining simulation parameters are as in Fig. 1.

as $(\sigma/b)^2$, that is to any asymmetric subthreshold ST in the regime of strong drive. Moreover, the synchronization mechanism underlying SR is revealed by the σ and Ω dependence of the return time distributions $N_2(T)$ more effectively, i.e., over a wider amplitude range, than by the corresponding spectral properties of the peak strengths $S(n\Omega)$. As an important difference with the weak drive case $A_0/b \ll (\sigma/b)^2 \ll 1$, we remark that the average residence times $\langle T_\pm \rangle$ that enter our synchronization conditions are (nonlinear) functions of the forcing amplitude, at variance with the linear response theory prescription, that for vanishingly small modulations the relaxation time constants are noise controlled, only. The dependence of $\langle T_\pm \rangle$ on A_0 for different values of the noise intensity is shown in Fig. 9.

V. CONCLUSIONS

The study of an asymmetric subthreshold Schmitt trigger driven by a sinusoidal signal with amplitude A_0 much larger than any internal noise intensity σ, that is $(\sigma/b)^2 \ll A_0/b < 1$, allowed us to underline the role of synchronization as a key mechanism in the SR phenomenology. In particular, we have shown the following.

(i) The residence time distributions $N_1(T)$ provide a reliable characterization of SR in a strongly driven symmetric device, at variance with claims to the contrary [11]. Each $N_1(T)$ peak strength P_n exhibits a SR maximum both as a function of the noise intensity σ and the forcing frequency Ω, according to the synchronization condition $\langle T_\pm \rangle = (n+1/2)T_\Omega$.

(ii) The output spectral power densities of an asymmetric device show δ-like peaks at the even harmonics, too. The strengths of the spectral peaks $S(n\Omega)$ with $n>1$ bear $[(n+1)/2]$ maxima versus the asymmetry parameter ϵ, according to the trigonometric condition (3.2). The optimal synchronization condition (3.1) proposed in Ref. [6] has been replaced by the weaker condition that $\langle T_+ \rangle + \langle T_- \rangle$ is (almost) independent of ϵ.

(iii) The return time distributions $N_2(T)$ yield an alternative characterization of SR in an asymmetric device. The resonance condition for the nth N_2 peak strength reads $\langle T_+ \rangle + \langle T_- \rangle = nT_\Omega$. The choice of the return time as the most significant switch time allowed us to circumvent the technical difficulties that might restrict the applicability of the synchronization-based definition of SR to symmetric systems, only.

Finally, the scaling law of Fig. 1 proves that in the strong drive regime the synchronization mechanism gets enhanced over the signal amplification mechanism, which, indeed, controls the onset of SR in weakly driven devices (i.e., in linear response theory approximation).

ACKNOWLEDGMENTS

The work was supported in part by the Istituto Nazionale di Fisica Nucleare (VIRGO Project). The authors wish to thank A. R. Bulsara, L. Gammaitoni, and P. Jung for stimulating discussions and helpful advice.

[1] J. Millman, *Microelectronics* (McGraw-Hill, New York, 1983).
[2] L. Gammaitoni, P. Hänggi, P. Jung, and F. Marchesoni, Rev. Mod. Phys. **70**, 223 (1998).
[3] S. Fauve and F. Heslot, Phys. Lett. **97A**, 5 (1983).
[4] B. McNamara and K. Wiesenfeld, Phys. Rev. A **39**, 4854 (1989).
[5] V. I. Melnikov, Phys. Rev. E **48**, 2481 (1993).
[6] A. R. Bulsara, M. E. Inchiosa, and L. Gammaitoni, Phys. Rev. Lett. **77**, 2162 (1996).
[7] F. Marchesoni, F. Apostolico, L. Gammaitoni, and S. Santucci, Phys. Rev. E **58**, 7079 (1998).
[8] P. Jung and P. Talkner, Phys. Rev. E **51**, 2640 (1995).
[9] P. Jung and P. Hänggi, Phys. Rev. A **44**, 8032 (1991).
[10] L. Gammaitoni, F. Marchesoni, and S. Santucci, Phys. Rev. Lett. **74**, 1052 (1995).
[11] M. H. Choi, R. F. Fox, and P. Jung, Phys. Rev. E **57**, 6335 (1998). In our simulations, the relevance of the $N_1(T)$ background to the determination of P_n could be assessed numerically in the weakly driven limit $A_0/b \ll (\sigma/b)^2 \ll 1$, only.
[12] P. Jung (private communication).
[13] P. Jung, Phys. Rep. **234**, 175 (1993).
[14] A. Longtin, A. R. Bulsara, and F. Moss, Phys. Rev. Lett. **67**, 656 (1991).